

The structure was determined by direct methods; hydrogen atoms bonded to carbon were placed in calculated positions. The solvent molecules were disordered over a center of symmetry and refined to 50% occupancy with the carbon of methanol and a chlorine of chloroform occupying the same site. Hydrogen atoms on N(13) and O(12) were located from a difference Fourier map and refined at 50% occupancy with constrained bond lengths and thermal parameters. All nonhydrogen atoms were refined anisotropically, whereas solvent atoms and hydrogen atoms were refined isotropically to a final *R* value of 0.078. The coordinates and other crystallographic details for all three structures have been deposited with the Cambridge Crystal-

- lographic Database.
14. S. Du Pre and H. Mendel, *Acta Crystallogr.* **8**, 311 (1955).
 15. A. R. Butler and C. Glidewell, *J. Chem. Soc. Perkin Trans. II* **1985**, 1465 (1985).
 16. G. L. Kenyon and G. L. Rowley, *J. Am. Chem. Soc.* **93**, 5552 (1971).
 17. A similar situation occurs in 2-cyanoguanidine, in which all C–N bonds of the guanidine moiety have nearly the same length [F. L. Hirshfeld and H. Hope, *Acta Crystallogr. B* **36**, 406 (1980)].
 18. J. J. P. Stewart, *MOPAC93* (Fujitsu, Tokyo, 1993).
 19. D. E. Koshland Jr., *Proc. Natl. Acad. Sci. U.S.A.* **44**, 98 (1958).
 20. W. P. Jencks, *Catalysis in Chemistry and Enzymol-*

ogy (Dover, New York, 1987), chap. 5; J. Kraut, *Science* **242**, 533 (1988).

21. P. Bühlmann and W. Simon, *Tetrahedron* **49**, 7627 (1993); D. L. Beckles *et al.*, *ibid.* **51**, 363 (1995).
22. We thank D. Nellis and M. Rickenbach for technical assistance with x-ray crystallography at Stony Brook and A. Richards (Molecular Simulations) for help with color graphics. We are grateful to Bayer Corporation for supporting this project and to the North Atlantic Treaty Organization for funding a travel grant for collaboration between two of the authors (T.W.B. and M.G.B.D.).

15 February 1995; accepted 6 June 1995

Molecular Diffuse Interstellar Band Carriers in the Red Rectangle

P. J. Sarre,* J. R. Miles, S. M. Scarrott

High-resolution optical spectroscopic observations of unidentified emission bands from the unusual biconical nebula known as the Red Rectangle are reported. The peak wavelengths and the widths of prominent bands near 5799, 5853, and 6616 angstroms decrease with increasing offset from the central A0-type star HD 44179 and, in the limit of large distance from the star, are shown to converge toward the known values for some of the narrower diffuse interstellar absorption bands at 5797, 5850, and 6614 angstroms. The same carriers give rise to both Red Rectangle emission and corresponding diffuse interstellar absorption bands, and these particular bands arise from electronic transitions in gas-phase molecules.

The identification of the carriers of the diffuse interstellar absorption bands is one of the most challenging astrophysical problems of this century. A large number of bands have been discovered (1), and their relative strengths, their widths, and in a few cases their shapes (2) have been characterized. Evidence in favor of free molecules as carriers has grown in recent years, but there is as yet no proof as to whether the bands originate in dust grains or molecules. There has also been a lack of any spectroscopic patterns that might guide laboratory-based experiments. A step forward was made with the recognition (3, 4) that some of the more prominent emission bands observed from the Red Rectangle appear to arise from the same carriers as a subset of the diffuse band carriers (5). Similar emission bands have also recently been detected in the carbon-rich R CrB star V854 Cen during minimum light (6). We report here high-resolution and high signal-to-noise optical spectra of the Red Rectangle that show conclusively that the Red Rectangle emission and complementary diffuse interstellar absorption bands arise from the same carriers and that these particular diffuse bands arise from electronic transitions in free, but as yet unidenti-

fied, gas-phase molecules. In addition, the results provide clear support for the idea of "families" of diffuse bands, demonstrate that some of the diffuse band carriers fluoresce, and open up new opportunities for laboratory study through the search for molecular emission spectra.

The Red Rectangle is a biconical nebula that is seen in both reflection and emission. The reflected component arises from light from the central star HD 44179 scattered by dust grains in the extended nebular medium. The optical emission consists of a broad red component [extended red emission (ERE)] on which is superimposed a remarkable spectrum of unidentified emission bands that are also excited by light from the central star (7–9), probably through a resonance fluorescence mechanism such as occurs in comets. Recent observations confirm that HD 44179 is a binary system (10), and a plausible scenario is that one component acts as the illumination source for material emanating from one star or possibly from both stars.

Earlier studies of the ultraviolet-visible and infrared (IR) spectra of the nebula have revealed a range of unusual aspects, including emission lines of Na D, Ca II H and K, H α (8), and the CO (11) and CH⁺ (12) molecules; there is also strong ERE (13) and a prominent set of "unidentified" IR bands (14), both of which probably arise from polycyclic aromatic hydrocarbon (PAH) material or molecules (15). Very striking, however,

is the set of strong optical emission bands, the most prominent of which fall near 5799, 5853, and 6616 Å, that lie close in wavelength to those of some strong, relatively narrow diffuse absorption bands ($\lambda=5797$, $\lambda=5850$, and $\lambda=6614$, where λ indicates the nominal wavelength); these diffuse bands have been linked into a "family" (16) on the basis of their common relative absorption strengths along various lines of sight.

Our data covering the region from 5100 to 6900 Å were recorded with the RGO spectrograph on the 3.9-m Anglo-Australian telescope at a resolution of 0.64 Å and with the slit of width 150 μm aligned along the northwest-southeast whisker at position angle 162°. A comparison between the 5800 Å region of the Red Rectangle at intermediate offset (centered at 7.5 arc sec) and the diffuse interstellar band absorption spectrum along the line of sight toward the heavily reddened star HD 183143 is shown in Fig. 1. The narrow $\lambda=5797$ and $\lambda=5850$ diffuse interstellar bands lie on the short-wavelength edge of the corresponding broader Red Rectangle fea-

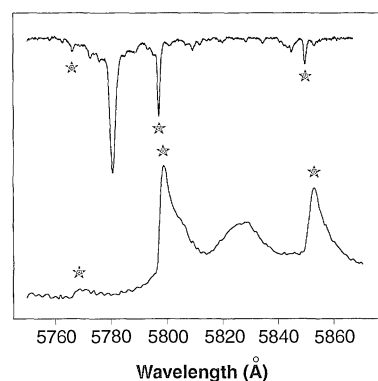


Fig. 1. Comparison between the diffuse absorption band spectrum toward HD 183143 (upper curve) (25) and the Red Rectangle spectrum (lower curve) in the 5800 Å region. Note the correspondence between the diffuse band and Red Rectangle features near 5769, 5799, and 5853 Å (stars), and the absence of Red Rectangle emission in the region of the $\lambda=5780$ diffuse band, which falls in a different family (16). The Red Rectangle data are the summed spectra for the region 5 to 10 arc sec offset from HD 44179 recorded with an integration time of 7200 s.

P. J. Sarre and J. R. Miles, Department of Chemistry, University of Nottingham, University Park, Nottingham NG7 2RD, UK.

S. M. Scarrott, Physics Department, University of Durham, South Road, Durham, DH1 3LE, UK.

*To whom correspondence should be addressed.

tures. In addition, these data show a further correspondence between an emission band near 5769 Å and a weak diffuse band near 5766 Å (17–19) that is well correlated with the strength of $\lambda=5797$ and therefore likely falls within the same family (16). The $\lambda=5797$ diffuse band and the corresponding Red Rectangle emission band have a similar profile, consisting of a steep short-wavelength side and an extended tail to longer wavelengths (2, 3, 5).

Our measurements of the peak wavelengths and widths of three of the most prominent Red Rectangle bands as a function of distance from HD 44179 (Fig. 2, A through C) show that they decrease with increasing distance from the star, and most notably, the Red Rectangle data converge toward the characteristics of the respective diffuse bands

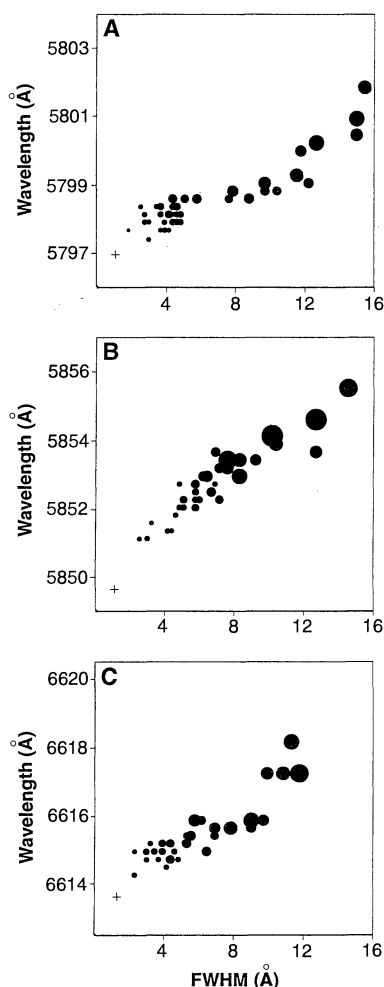


Fig. 2. Peak wavelength versus width [full width at half maximum (FWHM)] data for the three most prominent Red Rectangle bands near (A) 5799 Å, (B) 5853 Å, and (C) 6616 Å, with a velocity shift for nebular species taken from (10). The diameter of each circle is inversely proportional to the distance from the star HD 44179; smaller circles therefore represent cooler conditions. The cross marks the rest wavelength and width for the corresponding diffuse band toward HD 183143 (26).

in the limit of large distance from the star. Under these cooler conditions, the spectral characteristics of the emission bands are expected to match most closely those found in diffuse interstellar clouds. From this extrapolation, we conclude that the same carriers give rise to the corresponding pairs of emission and absorption bands. This does not mean that all of the bands under consideration ($\lambda=5797$, $\lambda=5850$, and $\lambda=6614$, and so forth) arise from a single carrier. The relative intensities within the group of emission bands near 5800 Å do not, however, appear to vary greatly with position in the nebula, and so it seems likely that these arise in one carrier.

The evolution of the bands in the 5800 Å and 6616 Å regions as a function of distance from HD 44179 is shown in Fig. 3, A and B,

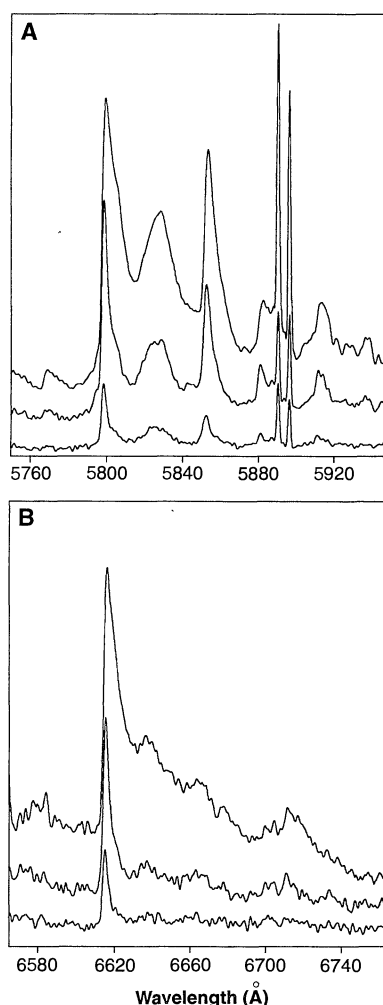


Fig. 3. Spectra of the Red Rectangle in the (A) 5800 Å and (B) 6616 Å regions at three different offsets from HD 44179 [7 (upper), 12 (middle), and 17 (lower) arc sec] showing the evolution of the band shapes. The emission bands appear on top of a broad background (ERE) that has been removed; each spectrum is offset on the vertical scale by an arbitrary amount, and the upper trace in each case is scaled by $\times 0.4$. The Na D lines are present in emission.

respectively. The spectra have the appearance of vibrational band structure, and the behavior of individual profiles is typical of the development of an unresolved rotational line contour as a function of temperature, which in this case is determined by the distance from the hot central star. The most likely interpretation is that the steep short-wavelength side of the 5799 Å feature is a rotational branch head and that a significant part of the red-degraded tail is the extension of the rotational branches to longer wavelengths. This is characteristic of a molecule for which one of the rotational constants is smaller in the excited state than in the ground electronic state.

A significant contribution to the intensity of the redward wing may arise from vibrational sequence band structure. Additional weaker diffuse bands in the 5800 Å region that also appear to correlate well with the Red Rectangle emission features have recently been reported; in particular, diffuse bands at 5818 Å (18, 19), 5828 Å (18, 19), and 5910 Å [see figures 4 and 6 in (19)] are close in wavelength to Red Rectangle features at 5819 Å (shoulder), 5828 Å, and 5912 Å (20).

The bands described here have not been reported in gas-phase laboratory experiments, but the fact that these “diffuse band” molecules have an emission spectrum is of considerable significance for future observational and laboratory studies. Laboratory-based detection of spectroscopic transitions in emission is more sensitive than in absorption, particularly through laser-induced fluorescence techniques. Rotational contour modeling can also be used to reduce the range of candidate molecular carriers.

Theoretical work (5) has indicated that the Red Rectangle 5799 Å feature and corresponding $\lambda=5797$ diffuse band could be accounted for in terms of an electronic transition in a large molecule, such as a C_{60} -based species, although not neutral C_{60} itself. However, from these data the most common observed intervals between the bands appear to be too low to correspond to vibrational excitations in a C_{60} -based molecule.

Although the solution to the problem of the Red Rectangle diffuse bands likely rests with the identification of new, possibly PAH-type (21), linear (8, 22), or ring carbon-based molecules, we note also that the rotational branch structure of even quite small open-shell molecules can be complex, and so an origin in a smaller molecule cannot yet be totally ruled out. Some consideration has been given, for example, to the CrO molecule as a carrier of the emission bands (23). As pointed out more than 10 years ago (7), the astrophysically important C_3 molecule has a spin-forbidden transition observed in emission in a matrix that falls

within the range of the 5800 Å bands; unfortunately, it has yet to be observed in the gas phase. The failure to detect C₃ in absorption in diffuse clouds (24), however, appears to rule out this attribution.

Note added in proof: We recently received a manuscript by R. J. Glinski and J. A. Nuth (27) in which a vibrational band assignment of the 5800 Å Red Rectangle emission features to C₃ is presented. Combining this assignment with the results described here leads to the conclusion that C₃ is the carrier of the $\lambda=5797$, $\lambda=5850$, and nearby related diffuse interstellar absorption bands.

REFERENCES AND NOTES

1. G. H. Herbig, *Astrophys. J.* **196**, 129 (1975); _____ and K. D. Leka, *ibid.* **382**, 193 (1991), and references therein; P. Jenniskens and F.-X. Désert, *Astron. Astrophys. Suppl. Ser.* **106**, 39 (1994).
2. B. E. Westerlund and J. Krelowski, *Astron. Astrophys.* **189**, 221 (1988); *ibid.* **203**, 134 (1988).
3. P. J. Sarre, *Nature* **351**, 356 (1991).
4. S. J. Fossey, *ibid.* **353**, 393 (1991).
5. S. M. Scarrott, S. Watkin, J. R. Miles, P. J. Sarre, *Mon. Not. R. Astron. Soc.* **255**, 11p (1992).
6. N. K. Rao and D. L. Lambert, *ibid.* **263**, L27 (1993).
7. G. D. Schmidt, M. Cohen, B. Margon, *Astrophys. J.* **239**, L133 (1980).
8. R. F. Warren-Smith, S. M. Scarrott, P. Murdin, *Nature* **292**, 317 (1981).
9. G. D. Schmidt and A. N. Witt, *Astrophys. J.* **383**, 698 (1991).
10. H. Van Winkel, C. Waelkens, L. B. F. M. Waters, *Astron. Astrophys.* **293**, L25 (1995).
11. M. L. Sitko, *Astrophys. J.* **265**, 848 (1983).
12. S. P. Balm and M. Jura, *Astron. Astrophys.* **261**, L25 (1992); D. I. Hall, J. R. Miles, P. J. Sarre, S. J. Fossey, *Nature* **358**, 629 (1992).
13. A. N. Witt and T. A. Boroson, *Astrophys. J.* **355**, 182 (1990).
14. R. W. Russell, B. T. Soifer, S. P. Willner, *ibid.* **220**, 568 (1978), and references therein.
15. D. G. Furton and A. N. Witt, *ibid.* **415**, L51 (1993); K. Sellgren, in *Dusty Objects in the Universe*, E. Bussoletti and A. A. Vittone, Eds. (Kluwer Academic, Dordrecht, Netherlands, 1990), pp. 35–47.
16. J. Krelowski and G. A. H. Walker, *J. R. Astron. Soc. Can.* **80**, 274 (1986); *Astrophys. J.* **312**, 860 (1987).
17. G. Chlewicki et al., *Astron. Astrophys.* **173**, 131 (1987).
18. P. Jenniskens and F.-X. Désert, *ibid.* **274**, 465 (1993).
19. J. Krelowski and C. Sneden, *Publ. Astron. Soc. Pac.* **105**, 1141 (1993).
20. A spectroscopic interpretation and modeling of these data will be described elsewhere (J. R. Miles, S. M. Scarrott, P. J. Sarre, in preparation).
21. G. P. Van der Zwet and L. J. Allamandola, *Astron. Astrophys.* **146**, 76 (1985); A. Léger and L. B. d'Hendecourt, *ibid.*, p. 81.
22. A. E. Douglas, *Nature* **269**, 130 (1977); J. K. G. Watson, *Astrophys. J.* **437**, 678 (1994).
23. P. D. Bennett, *Bull. Am. Astron. Soc.* **19**, 761 (1987).
24. T. P. Snow, C. G. Seab, C. L. Joseph, *Astrophys. J.* **335**, 185 (1988).
25. G. H. Herbig, personal communication.
26. _____, *Annu. Rev. Astron. Astrophys.*, in press.
27. R. J. Glinski and J. A. Nuth, in preparation.
28. We thank the Panel for the Allocation of Telescope Time for observing time on the Anglo-Australian Telescope and J. Bailey for assistance with the observations. The work of J.R.M. was funded under a fellowship of the Particle Physics and Astronomy Research Council. We thank R. J. Glinski and J. A. Nuth for sending us a copy of their manuscript and G. H. Herbig for permission to reproduce the diffuse absorption band spectrum in Fig. 1.

13 March 1995; accepted 23 May 1995

Decadal Trends in the North Atlantic Oscillation: Regional Temperatures and Precipitation

James W. Hurrell

Greenland ice-core data have revealed large decadal climate variations over the North Atlantic that can be related to a major source of low-frequency variability, the North Atlantic Oscillation. Over the past decade, the Oscillation has remained in one extreme phase during the winters, contributing significantly to the recent wintertime warmth across Europe and to cold conditions in the northwest Atlantic. An evaluation of the atmospheric moisture budget reveals coherent large-scale changes since 1980 that are linked to recent dry conditions over southern Europe and the Mediterranean, whereas northern Europe and parts of Scandinavia have generally experienced wetter than normal conditions.

A major source of interannual variability in the atmospheric circulation is the North Atlantic Oscillation (NAO) (1), which is associated with changes in the surface westerlies across the North Atlantic onto Europe (2). An index of the NAO reveals its variability since 1864 (Fig. 1A). The changes in circulation associated with changes in the NAO index are determined from the difference in sea-level pressure (SLP) between winters with an index value greater than 1.0 and those with an index value less than -1.0 (Fig. 1B). Differences of more than 15 mbar occur across the North Atlantic, with higher than normal pressures south of 55°N and a broad region of anomalously low pressure across the Arctic. During high NAO winters, the westerlies onto Europe are over 8 m s⁻¹ stronger than during low NAO winters (Fig. 1B), anomalous southerly flow occurs over the eastern United States, and anomalous northerly flow occurs across western Greenland, the Canadian Arctic, and the Mediterranean.

In addition to interannual variability, there have been several periods (Fig. 1A) when such anomalous circulation patterns persisted over many winters. In the region of the Icelandic low, seasonal pressures were anomalously low during wintertime from the turn of the century until about 1930, while pressures were higher than normal at lower latitudes. Consequently, the wind across the North Atlantic had a strong westerly component, and the moderating influence of the ocean contributed to warmer than normal winter temperatures over much of Europe (3). From the early 1940s until the early 1970s, when the NAO index exhibited a downward trend, European wintertime temperatures were frequently lower than normal (4, 5). A sharp reversal has occurred over the past 25 years, with unprecedented strongly positive NAO index values since 1980 and with SLP anomalies much like those shown in Fig. 1B. The 1983, 1989, and

1990 winters were marked by the highest positive values of the NAO index recorded since 1864.

Variations in the quasistationary planetary waves in the atmosphere, among other factors, produce spatially coherent large-scale patterns of anomalies in local surface variables on interannual and longer time scales (4, 6). Such patterns can be observed in the surface temperature and sea-surface temperature (SST) anomalies (7) for the period from 1981 to 1993 (Fig. 2). The general pattern has been one of cooling over the oceans and warming over the continents. The North Pacific basin temperature anomalies, with warming along the west coast of North America and Alaska and cooling in the central North Pacific, have been linked to a substantial decadal change in the atmospheric circulation, which corresponded to a deepened eastward-shifted Aleutian low pressure system during the winter half of the year and lasted throughout most of the 1980s (8, 9). Changes in the mean flow were accompanied by a southward shift in the storm tracks and associated synoptic eddy activity (9) and in surface ocean sensible and latent heat fluxes (10). It has been hypothesized that the Pacific decadal time scale variation has its origin in the tropics (9), and several modeling studies have confirmed that North Pacific atmospheric circulation changes are controlled in part by anomalous tropical Pacific SST forcing (11, 12).

Decadal changes in the atmospheric circulation and lower tropospheric temperatures during winter over the North Atlantic and adjacent land areas, however, do not appear to be as strongly influenced by tropical Pacific SST variability (12, 13). The anomalous coldness over the past decade near Greenland and the eastern Mediterranean, and the very warm conditions over Scandinavia, northern Europe, the former Soviet Union, and much of central Asia (Fig. 2), are more strongly linked to the recent behavior of the NAO. To isolate the important coupled modes of variability between the SLP and surface temperature and

National Center for Atmospheric Research, P.O. Box 3000, Boulder, CO 80307, USA.